JOURNAL OF RAMAN SPECTROSCOPY
J. Raman Spectrosc. 2002; **33**: 498–502
Published online in Wiley InterScience (www.interscience.wiley.com). DOI: 10.1002/jrs.903

JRS

Near-infrared multichannel Raman spectroscopy toward real-time *in vivo* cancer diagnosis

Shoji Kaminaka,[1] Toshiaki Ito,[2] Hiroya Yamazaki,[3] Ehiichi Kohda[3] and Hiro-o Hamaguchi[1]*

[1] Department of Chemistry, School of Science, The University of Tokyo, 7-3-1 Hongo, Bunkyo-ku, Tokyo 113-0033, Japan
[2] Hamamatsu Photonics Co. Ltd, 5000 Hirakuchi, Hamakita, Shizuoka 434-8601, Japan
[3] Department of Radiology, School of Medicine, Keio University, 35 Shinanomachi, Shinjuku-ku, Tokyo 160-8582, Japan

Received 19 October 2001; Accepted 17 April 2002

Using a newly developed InP/InGaAsP multichannel detector, we developed a near-infrared Raman spectroscopic system that can measure human tissues efficiently without interference from fluorescence. This enabled us to measure an *in vivo* Raman spectrum of live human tissue (skin) in 1 min using fiber probe optics. By applying this system to human lung tissues, we found that Raman spectroscopy makes a clear distinction not only between normal and cancerous tissues but also between two different types of lung carcinomas. The results indicate a promising future for the non-invasive real-time Raman diagnosis of cancers. Copyright © 2002 John Wiley & Sons, Ltd.

INTRODUCTION

Vibrational Raman spectra are often called 'molecular fingerprints' owing to their high specificity to molecular structure.[1,2] They provide useful information on the molecular composition of human tissues,[3,4] permitting the unambiguous differentiation of cancerous and normal tissues.[5–16] There has been keen interest in the last decade in the potential of molecular-level cancer diagnosis by Raman spectroscopy. However, human tissues irradiated by laser light often emit fluorescence, which ruins entirely the otherwise useful Raman spectrum. In order to bypass the problem of fluorescence, near-infrared excitation around 800 nm has been used with Si charge-coupled device (CCD) detectors.[7,8,10,11,15,17–20] However, some human tissue samples emit fluorescence even if they are excited at 800 nm.[11,21] Since the longest excitation wavelength practicable with an Si CCD detector is ~850 nm, a new detector sensitive in the deep near-infrared region has been sought. We recently demonstrated, using an InP/InGaAsP photomultiplier, that excitation at 1064 nm was highly effective for eliminating fluorescence from the Raman spectra of human lung tissues,[22] although a long accumulation time of several hours was inevitable. In this paper, we show that we are now able to shorten the measurement time to a few minutes, thanks to a new InP/InGaAsP near-infrared multichannel detector. We also show that the high efficiency of the present system makes it possible to measure an *in vivo* Raman spectrum of a live human tissue (skin) in 1 min using a fiber Raman probe.

*Correspondence to: Hiro-o Hamaguchi, Department of Chemistry, School of Science, The University of Tokyo, 7-3-1 Hongo, Bunkyo-ku, Tokyo 113-0033, Japan.
E-mail: hhama@chem.s.u-tokyo.ac.jp

EXPERIMENTAL

Near-infrared Raman measurements

The setup of our near-infrared Raman system is shown schematically in Fig. 1. A quasi-continuous Q-switched Nd : YAG laser (Spectra-Physics X30-106Q, wavelength 1064 nm, repetition rate 25 kHz, pulse duration 100 ns) was used as a near-infrared Raman excitation source. An He–Ne laser beam (power ~1 mW) was overlapped with the 1064 nm beam (power ~110 mW) in order to visualize the Raman sampling spot. The 1064 nm laser beam was focused on an area of 1 mm × 100 μm by two cylindrical lenses (f = 150 and 80 mm) for the 180° backscattering configuration [Fig. 1(a)]. Raman scattered light was collected by a collimating lens and focused on the entrance slit of the polychromator through two holographic notch filters (Kaiser). An InP/InGaAsP near-infrared multichannel detector (Hamamatsu Photonics, intensified diode array with 180 effective channels, quantum efficiency ~1% for 1–1.4 μm) was used. In order to eliminate thermal noise, the multichannel detector was gated (100 ns gate width), synchronizing with the Nd : YAG laser pulse. A visible-cut filter (CVI Laser RG-850, transparent for $\lambda > 850$ nm) was placed behind the entrance slit so as to avoid contamination with room light. The spectral resolution was ~10 cm^{-1}. All Raman spectra were obtained with a 400 s exposure time, except for the measurement of human skin, where a 64 s exposure was used. A 6 + 1 fiber Raman probe, 2 m long and made of seven low-OH silica fibers (numerical aperture ~0.2) of 400 μm diameter,

was also used [Fig. 1(b)]. It consisted of a central fiber for Raman excitation and six Raman collecting fibers surrounding it. The output ends of the six Raman collecting fibers were aligned parallel to the entrance slit of a polychromator (ISA, TRIAX320, $f = 4.0$). The Raman probe was set 3 mm away from the sample surface and the 1064 nm laser beam irradiated a circular area of 2 mm diameter in the fiber configuration.

Tissue samples

Dissection or open surgery specimens from seven patients (five adenocarcinomas and two squamous cell carcinomas) were used. Cubic tissue samples of $5 \times 5 \times 5$ mm cube were cut from each specimen, from both the cancerous and normal regions, and used for Raman measurements. Three different spots of each tissue sample were measured and a total of 21 Raman spectra were obtained for both the cancerous and normal tissues. All the specimens were stored for less than 1 year after resection in 10% formaldehyde aqueous solution. Raman measurements were carried out in a sample holder filled with the same formaldehyde aqueous solution. After the Raman measurements, pathologists reconfirmed the histopathological types for each of the tissue samples.

Data analysis

The observed Raman wavenumbers were calibrated by using the Raman spectrum of 4-dimethylamino-4′-nitroazobenzene. The sensitivity of the total Raman system was determined by recording a tungsten lamp. Curve-fitting analysis was performed after background subtraction by assuming a linear function for the background. Igor Pro 3.14 (WaveMetrics) was used for all analyses.

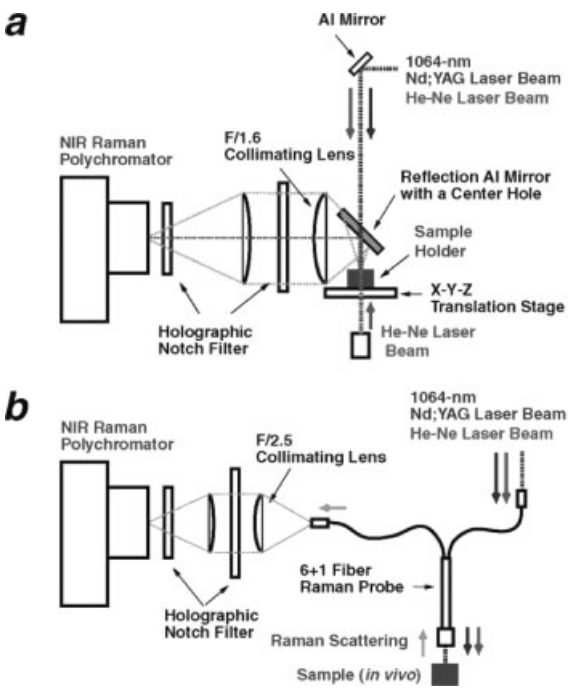

Figure 1. Optical layout of the near-infrared multichannel Raman system used in the present study. (a) Conventional 180° backscattering configuration; (b) *in vivo* 180° backscattering configuration with a $6 + 1$ fiber Raman probe.

RESULTS AND DISCUSSION

In order to show the high efficiency of the present near-infrared multichannel Raman system, in Fig. 2 we compare several Raman spectra of human lung tissues with and without cancer. All spectra in Fig. 2 are normalized so that spectral patterns and not the absolute intensities are compared. We note that Raman spectra of human lung tissues are obtainable only by means of near-infrared excitation at 1064 nm; excitation at shorter wavelengths causes a high fluorescence background that entirely masks the Raman spectrum. The spectra in Fig. 2(a) were obtained from lung squamous cell carcinoma tissues with single-channel detection using an InP/InGaAsP photomultiplier (1) and with multichannel detection using a new multichannel detector having the same photocathode (2). Although the measurement time is 36 times longer with single-channel detection (~240 min) than with multichannel detection (400 s), the signal-to-noise (S/N) ratio is about an order of magnitude better in multichannel detection. The high efficiency of the present multichannel system makes it possible to perform Raman spectroscopy with fiber optics, which is a requisite for practical *in vivo* clinical applications. We custom-made a $6 + 1$ fiber Raman probe which consisted of one Raman excitation fiber at the center and six Raman collection fibers surrounding it.[17–20] In Fig. 2(b) we compare the Raman spectra of a lung adenocarcinoma tissue measured under the same experimental conditions using the conventional 180° backscattering geometry (1) and the $6 + 1$ fiber Raman probe (2). The S/N ratios in these two spectra are comparable to each other, indicating that the optical loss in our $6 + 1$ fiber Raman probe is not problematic in *in vivo* Raman measurements. The *in vivo* capability of our system was further checked by measuring human skin. Figure 2(b)(3) shows the Raman spectrum of human skin measured with the fiber Raman probe with a measurement time of 64 s. Two characteristic Raman bands of collagen are observed with a good S/N ratio. These experimental results indicate that our near-infrared multichannel Raman system is already applicable to *in vivo* Raman measurements as it is. Furthermore, we anticipate an order of magnitude improvement in the quantum efficiency of the InP/InGaAsP photocathode in the near future; the quantum efficiency is now about 1% and a preliminary test has shown that it can be raised to 10% under optimized manufacturing conditions. We should be able to measure *in vivo* Raman spectra of live human tissues in real time in less than 10 s.

Now that real-time *in vivo* Raman measurements of human tissues are well within our reach, we would like to

JRS

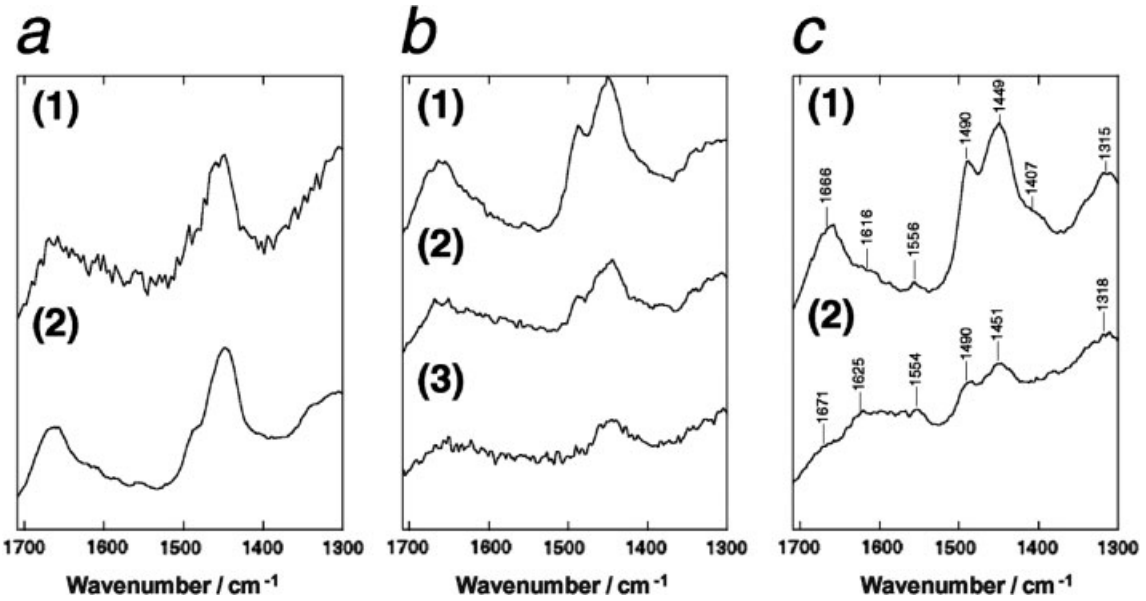

Figure 2. Raman spectra (1064 nm excitation) of human lung tissues. (a) Spectra of lung squamous cell carcinoma tissues obtained with (1) a single-channel detector (Hamamatsu R5509-42 InP/InGaAsP photomultiplier, accumulation time ~240 min) and (2) multichannel detection with the new InP/InGaAsP multichannel detector (400 s). (b) Spectra of a lung adenocarcinoma tissue obtained with (1) the conventional 180° backscattering configuration (400 s) and (2) the 6 + 1 fiber Raman probe (400 s). The *in vivo* Raman spectrum of human skin (Asian) measured with the fiber Raman probe (64 s) is also shown (3). (c) Spectra of (1) adenocarcinoma lung tissue and (2) normal lung tissue (400 s).

examine carefully the information contents of the Raman spectra, which are essential for highly reliable disease diagnosis. In Fig. 2(c) we compare the Raman spectra in the 1300–1710 cm^{-1} region of adenocarcinoma (1) and normal (2) human lung tissues. The two spectra show distinct spectral patterns, as already reported by many other groups.[5–16] Several Raman bands are observed commonly for the cancerous and normal tissues, including the bands assignable to the amide I (~1670 cm^{-1}) and the CH_2 bend (~1450 cm^{-1}) modes, but their relative intensities are different from each other. For diagnostic purposes, these spectral differences are highly meaningful in themselves, although assignments of all the observed Raman bands will be necessary for future pathological studies of cancers. Here, we do not go into the details of the vibrational assignments. We also note that the Raman spectrum of a squamous cell carcinoma tissue [Fig. 2(a)(2)] and that of an adenocarcinoma tissue [Fig. 2(b)(1)] are very similar to each other, with a small difference in the relative intensities of the 1490 and 1449 cm^{-1} bands. It is straightforward to make a distinction between the cancerous and normal states by Raman spectroscopy, but further spectral analysis is indispensable if squamous cell carcinoma is to be differentiated from adenocarcinoma.

For more detailed spectral analysis, Fig. 3(a) shows two representative Raman spectra in the 1500–1700 cm^{-1} wavenumber region of cancerous (adenocarcinoma) and normal lung tissues. This wavenumber region can be measured simultaneously by one exposure. We also measured the other wavenumber regions by shifting the center wavelength of the polychromator and found that this region is the most sensitive for the differentiation of normal and cancerous tissues. By a curve-fitting analysis using Gaussian functions, we can resolve the observed features in Fig. 3(a) and (b) into five components, bands 1–5. In this fitting analysis, we first obtained the average spectra of the normal and cancerous spectra by simply averaging the data and decomposed the averaged spectra by a least-squares fitting analysis. We needed at least five components to fit the average spectra. Each Raman spectrum was then fitted using the five components in the averaged spectra as the initial parameters. Although band 4 is necessary to produce a small peak at ~1575 cm^{-1} in the normal tissue spectrum, the general trends of the two spectra are well reproduced by bands 1, 2, 3 and 5. We use band 1 as the intensity standard, and quantify the spectral differences using the relative intensity of band 5 to band 1 and that of (band 2 + band 3) to band 1. Because the observed features consisting of bands 2 and 3 are very broad, we analyze the combined intensity (band 2 + band 3) rather than using band 2 and band 3 separately, so that the arbitrariness of band decomposition does not affect the results seriously. A two-dimensional correlation plot of the two relative intensities is shown in Fig. 3(b). A total of 42 points (21 from cancerous and 21 from normal tissues) corresponding to 42 Raman spectra are plotted, with open circles indicating points obtained from normal lung tissues, open squares from adenocarcinoma tissues and filled squares from

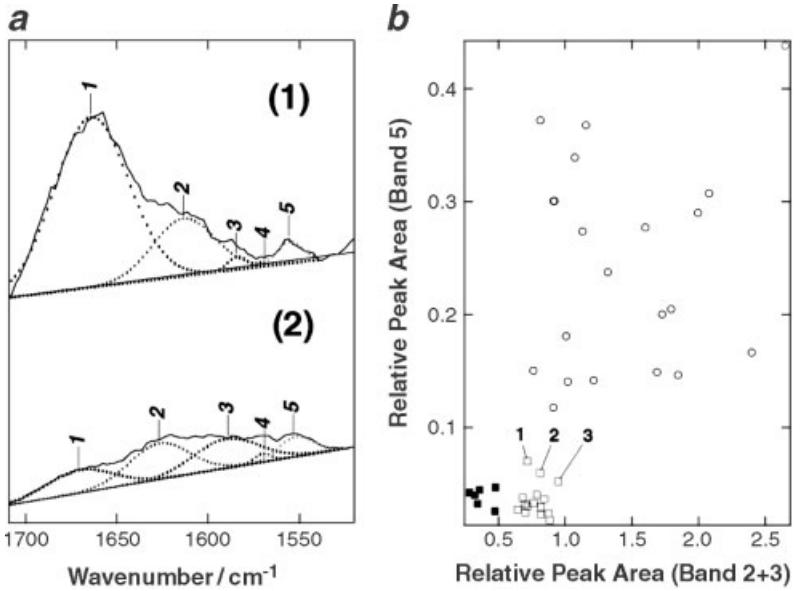

Figure 3. Curve-fitting analysis of the Raman spectra of the cancerous and normal lung tissues. (a) Curve-fitting decomposition of Raman spectra in the 1500–1700 cm^{-1} region of adenocarcinoma tissue (1) and normal tissue (2). Five Gaussian bands, bands 1–5, are used for decomposition. (b) Two-dimensional correlation plot of relative intensities band 5/band 1 vs (band 2 + band 3)/band 1. Open-circles, normal tissue; open squares, adenocarcinoma tissue; closed-squares, squamous cell carcinoma tissue.

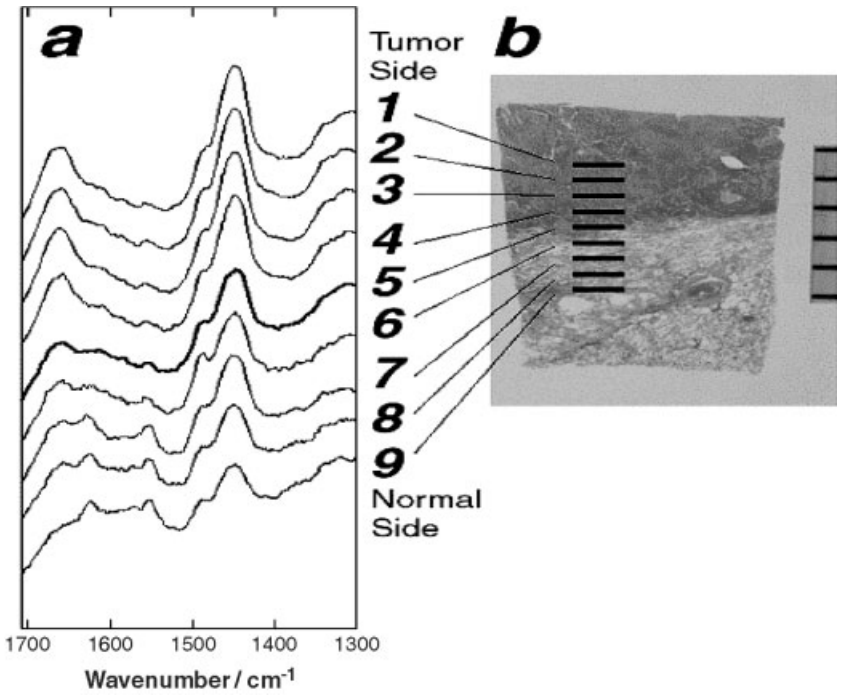

Figure 4. Raman spectra of human lung tissue measured at nine different spots at intervals of 500 μm from the tumor side to the normal side. (a) Spectra at the nine spots indicated in (b). (b) Enlarged image of hematoxylion and eosin-stained human lung tissue. The dark area is due to the stained squamous cell carcinoma. The ruler on the right measures 1 mm with digits. Thick horizontal bars indicate the Raman sampling spots.

squamous cell carcinomas tissues. The two-dimensional plot clearly separates the normal and cancerous Raman spectra and also those of adenocarcinoma and squamous cell carcinoma tissues. The plot even separates adenocarcinoma containing connective tissue (open squares 1, 2 and 3) from full adenocarcinoma. These pieces of evidence strongly suggest that the Raman spectra are informative enough to make a distinction not only between normal and cancerous

tissues but also between cancerous tissues of different types. They also indicate that the two-dimensional correlation plot introduced here for the first time (multi-dimensional correlation plots in the future) is highly useful in Raman spectral analyses for disease diagnosis.

A further important factor that we have to examine is how precisely we can determine the tumor area by Raman spectroscopy. Although Raman spectroscopy achieves a high spatial resolution of less than 1 μm if a confocal Raman microscope[15,16,23,24] is employed, we here discuss the capability on a macroscopic scale of millimeters, which is practically important in surgery. Figure 4 shows a set of Raman spectra of lung tissues obtained from the same specimen but at different spots intersecting the border between the cancerous and normal regions. Macroscopic 180° backscattering geometry was used to focus the laser beam into a 1 mm × 100 μm area [horizontal bars in Fig. 4(b)]. Raman spectra were measured for nine different spots at intervals of 500 μm from the cancerous side to the normal side of the specimen. Spectrum 5 in Fig. 4(a) is the Raman spectrum on the border between the cancerous and normal regions and shows an intermediate pattern in the 1500–1700 cm^{-1} region. On the other hand, spectrum 3 shows a typical pattern of a cancerous tissue and spectrum 7 shows that of a normal tissue. Raman spectroscopy can identify the cancerous area in a tissue with a lateral spatial resolution of about 1 mm. We note that this spatial resolution is not limited by the instrument but is limited by the sample itself that has a rather obscured border between the cancerous and normal regions.

We have shown the experimental capability of our new near-infrared multichannel Raman system and the high information contents of Raman spectra obtained thereby for realizing non-invasive real-time diagnosis of cancers. The complete elimination of the fluorescence background from the original Raman spectra dramatically shortened the total time needed for cancer diagnosis, facilitating the analysis without any mathematical background subtraction. Most important, the possibility of distinguishing different types of cancers at a molecular level has been demonstrated for the first time. We are planning a feasibility test of this new diagnostic tool in the near future.

REFERENCES

1. Long DA. *Raman Spectroscopy*. McGraw-Hill: New York, 1977.
2. Herzberg G. *Molecular Spectra and Molecular Structure II. Infrared and Raman Spectra of Polyatomic Molecules*. D. Van Nostrand: New York, 1945.
3. Tu AT. *Raman Spectroscopy in Biology*. Wiley–Interscience: New York, 1982.
4. Spiro TG (ed.). *Biological Applications of Raman Spectroscopy*. Wiley: New York, 1987.
5. Liu C-H, Das BB, Glassman WLS, Tang GC, Yoo KM, Zhu HR, Akins DL, Lubicz SS, Cleary J, Prudente R, Celmer E, Caron A, Alfano RR. *J. Photochem. Photobiol. B* 1992; **16**: 187.
6. Lawson EE, Barry BW, Williams AC, Edwards HGM. *J. Raman Spectrosc.* 1997; **28**: 111.
7. Mahadevan-Jansen A, Mitchell MF, Ramanujam N, Malpica A, Thomsen S, Utzinger U, Richards-Kortum R. *Photochem. Photobiol.* 1998; **68**: 123.
8. Mahadevan-Jansen A, Mitchell MF, Ramanujam N, Malpica A, Thomsen S, Utzinger U, Richards-Kortum R. *Photochem. Photobiol.* 1998; **68**: 427.
9. Redd DCB, Feng ZC, Yue KT, Gansler TS. *Appl. Spectrosc.* 1993; **47**: 787.
10. Frank CJ, Redd DCB, Gansler TS, McCreery RL. *Anal. Chem.* 1994; **66**: 319.
11. Frank CJ, McCreery RL, Redd DCB. *Anal. Chem.* 1995; **67**: 777.
12. Boustany NN, Manoharan R, Dasari RR, Feld MS. *Appl. Spectrosc.* 2000; **54**: 24.
13. Gniadecka M, Wulf HC, Mortensen NN, Nielsen OF, Christensen DH. *J. Raman Spectrosc.* 1997; **28**: 125.
14. Gniadecka M, Wulf HC, Nielsen OF, Christensen DH, Hercogova J. *Photochem. Photobiol.* 1997; **66**: 418.
15. Hawi SR, Campbell WB, Kajdacsy-Balla A, Murphy R, Adar F, Nithipatikom K. *Cancer Lett.* 1996; **110**: 35.
16. Schut TCB, Puppels GJ, Kraan YM, Greve J, van der Maas LLJ, Figdor CG. *Int. J. Cancer* 1997; **74**: 20.
17. Brennan JF III, Wang Y, Dasari RR, Feld MS. *Appl. Spectrosc.* 1997; **51**: 201.
18. Shim MG, Wilson BC. *J. Raman Spectrosc.* 1997; **28**: 131.
19. Shim MG, Wilson BC, Marple E, Wach M. *Appl. Spectrosc.* 1999; **53**: 619.
20. Shim MG, Song L, Marcon NE, Wilson BC. *Photochem. Photobiol.* 2000; **72**: 146.
21. Cooney TF, Skinner HT, Angel SM. *Appl. Spectrosc.* 1996; **50**: 836.
22. Kaminaka S, Ito T, Yamazaki H, Kohda E, Hamaguchi H. *J. Raman Spectrosc.* 2001; **32**: 139.
23. Puppels GJ, Demul FFM, Otto C, Greve J, Robertnicoud M, Arndtjovin DJ, Jovin TM. *Nature (London)* 1990; **347**: 301.
24. Takai Y, Masuko T, Takeuchi H. *Biochim. Biophys. Acta* 1997; **1335**: 199.